PCCP

Tilting in Coronene Layers on Au(111)

Journal:	*Physical Chemistry Chemical Physics*
Manuscript ID	CP-ART-07-2020-003658.R3
Article Type:	Paper
Date Submitted by the Author:	07-Nov-2020

Complete List of Authors:	Kabat, Nathaniel; University of Virginia, Materials Science and Engineering Monazami, Ehsan; University of Virginia, Materials Science and Engineering Reinke, P; University of Virginia, Materials Science and Engineering

Tilting in Coronene Layers on Au(111)

Nathaniel W. Kabat, Ehsan Monazami, and Petra Reinke*

University of Virginia, Department of Materials Science and Engineering, 395 McCormick Road, Charlottesville, VA 22901, U.S.A.

E-mail: pr6e@virginia.edu

Abstract

Control of molecule adsorption and ordering on metal surfaces is of critical importance for the design and fabrication of molecule-based functional materials. In the present work the molecule layer structures of coronene on Au(111) and HOPG are studied by combining experiment using scanning tunneling microscopy, with image analysis techniques to unravel small changes in molecule adsorption geometry. Coronene forms a densely packed layer on Au(111) and HOPG at room temperature, but does not preferentially decorate the herringbone reconstruction. The molecule layer structure is confirmed by histograms of molecule radius and apparent height obtained from STM images using a python based, open source code. Annealing to 116°C initiates a tilting of coronene molecules on Au(111) by about 11±4° which is deduced from statistical image analysis. The structural analysis is combined with an assessment of apparent height modulation with bias voltage to ascertain reliability of the statistical analysis. Our work illustrates that the combination of advanced image analysis processing and STM images allow to extract even small changes in molecule layer structure.

Introduction

Coronene molecules ($C_{24}H_{12}$) have garnered attention in diverse field including graphene synthesis,[1–4] supramolecular chemistry and assembly,[5,6] and even superconductivity.[7,8] Coronene molecules are one of the smallest repeating molecular units with graphene lattice structure, and have consequently attracted interest as a model system,[9] and in the study molecule-surface interactions. Coronene is a polycyclic aromatic hydrocarbon and intermolecular interactions are solely due to van-der-Waals bonding. The structure of single and multilayer coronene depends sensitively on the molecule-substrate interaction which competes with the intermolecular forces.[10] Bulk coronene crystallizes in a monoclinic crystal structure and the molecules form stacks along the b-axis which are tilted with respect to each other optimizing inter-molecule interactions[11,12]

Coronene molecules are chemisorbed on Si(111) and lie flat on the surface, occupying specific sites due to their interaction with unsaturated bonds in the (7x7) reconstruction. The strong interaction with the Si surface also leads to slight buckling within the molecule, and long range order, which is driven by intermolecular interactions is suppressed.[13,14] This is in contrast to Ge, where the coronene molecules form a tilted adlayer, and a flat, weakly adsorbed second layer.[15,16] Coronene is van-der-Waals bonded to surfaces such as HOPG and MoS_2 and self-organizes in densely packed, well ordered layers.[17–20] The most commonly studied metal surfaces are Ag,[21–25] Au,[7,8,24,26–32] and Cu,[21,33] mostly for the (111) orientation. These weakly interacting Cor/metal systems show long range molecular order, but strongly interacting substrates such as Rh, Ir, and Ru, which are also commonly used for graphene synthesis, suppress long range ordering.[2,4] Ag(111) is somewhat intermediate between weak and strong adsorption and flat as well as tilted coronene orientations have been reported.[23,24] In Cor/Au(111) the molecular layer adopts a commensurate (4x4) surface structure,[26] which is not affected by the herringbone surface reconstruction. This system adopts a Stranski-Krastanov growth mode for multilayers, which is also seen on HOPG.[22] The majority of studies on the Cor/Au(111) system were performed in solution often with liquid-STM tech-

niques, and molecular ordering is then influenced by the interaction with the solvent and results cannot directly be compared with vacuum deposited materials.[27–32]

The assessment of molecular orientation (i.e. flat, upright, tilted) is vitally important to control materials properties and in particular charge transport in molecular adlayers. We seek to address this question for the Cor/Au(111) system[8,24] and observe the changes to its structure as a function of temperature, which can offer an additional control parameter for molecule layer structure. The temperature dependence of layer structure has so far only been considered in solution based experiments for Au(111)[28,29] and Ag(110)[25] substrates. We present study which combines STM/STS with statistical image analysis. Our work illustrates the onset of molecule tilting in response to annealing for Cor/Au(111). Deposition of coronene on HOPG (highly oriented pyrolitic graphite) was used for comparison. Open source Python libraries are used for image analysis, and offer in combination with STM insight in the details of the coronene layer structure.

Experimental

All experiments were performed under ultrahigh vacuum conditions (base pressure: $3x10^{-10}$ mbar) using an Omicron VT-STM (variable temperature-scanning tunneling microscope). Coronene (Sigma-Aldrich, 97.0% purity) was deposited using a homemade Knudsen-style deposition source and monitored by a standard Chromel-Alumel thermocouple. The source was degassed carefully prior to coronene deposition and the deposition rate was adjusted by variation of the source temperature. Sub-monolayer depositions in combination with STM imaging were used for calibration of the deposition rate. The substrate(s) were held at room temperature during deposition and the source was at 180°C ±5°C. Au(111) samples (Gold on Mica from Molecular Imaging), were annealed repeatedly in vacuum up to 500-600°C to desorb contamination and trigger surface reconstructions. HOPG samples were annealed overnight at 200-300°C in vacuum. To observe changes with anneal temperature,

Cor/Au(111) samples were heated to the specific temperature and cooled to room temperature before imaging. All STM measurements were done with electrochemically etched W tips. Typical Cor/Au(111) STM imaging conditions were $V_b = \pm 1.2$ V and $I_t = 0.04$-0.2 nA,V_b below 0.6 V did not yield any good images, albeit it was possible to image with lower V_b on the Cor/HOPG layers. The STM images have a slight distortion, which is seen in the FFT patterns included in Figures 3 and 4. However, the deviation from ideality, which is present in many STM images due to non-ideality of the piezoceramics, is identical in all our images, and we therefore decided not to use any corrections. The agreement in distortion across all our images also confirms that it is not induced by thermal drift. The dimensions of the molecule envelope summarized in the histograms included in Figures 1 and 5 agree well with expected values based on molecule geometry. The measurements of apparent height are not influenced by this distortion. Imaging (scanning) speed was held constant throughout the experiments, and measurements were performed near the center of the piezo-ceramic range. Automated (or semi-automated) image analysis enables us to extract small variation in surface structure and, in the present work, variations in molecule arrangement on a surface. However, the reliability, and hence also interpretability of the results relies on knowledge of all the factors which can lead to an undesirable modulation of the images. One well-known aspect is the change in apparent height as a function of bias voltage illustrated in Figure 7, which reflects on the local density of states in the molecules. In addition, the imaging speed as well as image size should be kept (near) constant, or the impact of these parameters on the image features has to be clearly understood and integrated in the image analysis and interpretation. Images can include shear or other systematic image modulation due to the performance of a specific piezo-ceramic element or other systematic, instrument specific errors. For this purpose we include in Figure 4 the FFT (Fast Fourier Transform) calculated from the respective STM images. The angles between the diffraction spots in the FFT were measured by marking the center of each diffraction spot. The variations in internal angles (counted clockwise) for images progressing from ambient temperature to 97°

C annealing to 116 °C annealing steps are: ±2°, ±1°, and ±2.5°, with the variation for the two highest temperatures being ±0.5°, ±0.5°, and ±1°. The error in the angle measurement overall is estimated to be about ±1° as determined from repeated sampling. The change in shear from image to image is largest for the two lowest temperatures with closely matched height and distance histograms, and the variation in shear is smaller for the two highest temperatures, where the height distributions indicate a change in molecule conformation or stacking. Hence, variations in image shear can not be held responsible for the observed modulation of the coronene layer with temperature. It will be important in the exploration of the limits and opportunities offered by automated image analysis to ascertain the possible impact of image distortions. In our case, the shear is rather small and we therefore did not use an image correction which can itself introduce artefacts.

Data Analysis

All STM images were analyzed using WSxM[34] and/or Gwyddion.[35] SPIW/SPIEPy[36,37] was used to determine topographic maximum/minimum positions. Sklearn[38] was applied to calculate nearest neighbor distances based on the distances between maxima and minima. The standard libraries for scientific computing/data analysis Scipy, Numpy, and Matplotlib were also applied The molecule spacing is defined as the distance between maximum positions where each maximum position represents a single molecule. The molecule radius is the distance between the the maximum position and the next nearest minimum. Each minimum position corresponds to the edge of the molecule which coincides with the physical gap between molecules defined by the hydrogen terminated perimeter. The height of a given molecule (h_{cor}) is calculated as the difference between measured STM height from molecule center to nearest minimum point. An example of this process is summarized in Figure 1.Note that all heights cited in this work are apparent heights since in STM height information is always convoluted with the local density of states. This is most readily apparent in Figure

7, where it is shown that apparent height is a function V_b (bias voltage). The minimum height position in the closed molecule layers corresponds to the hydrogen terminated rim of the coronene and not to the substrate surface. All "heights" cited in this manuscript should be understood as "apparent heights". The image analysis was first tested for Cor/HOPG which is known to adopt a flat configuration.[17]

Figure 1a shows a representative STM image as it was recorded for Cor/Au(111). The STM image is translated into a 2D array of molecule positions (Figure 1b). This 2D array in [x,y] format is referenced to values in the STM image, thus producing molecule height, molecule distance, and molecule radius values included in Figures 1c - d. A ball-and-stick model of coronene and its hexagonal envelope, which defines the molecule perimeter in the STM images, is also included (Figure 1e).The automatic detection of maxima and minima and their corresponding position within an image yields the distance histograms. Within some margin of error, these points should be positioned at the same physical symmetry point(s) on an individual coronene molecule. In the case of the highly symmetric coronene molecule the maxima are indeed positioned at the molecule center, but this is certainly not valid for all types of molecules and has to be tested for each material. The histograms shown in Figure 1d reflect the hexagonal shape of the molecule: the shortest distance from center to hexagon edge coincides with the lower distance limit in the histograms.

STM images are flattened, Gaussian smoothed, and masked to remove image aberrations introduced in the experiment from consideration in the image analysis. The SPIW/SPIEPy algorithm is suited for atomically flat high quality STM images with a large degree of periodicity (i.e. atomic or molecular surface structure). Due to streaks and other experimental imaging artifacts, which are quite common, the algorithm does not find a peak for every molecule in the image. The number of molecules per data point for the subsequent discussion is between 50-500 molecules depending on the scan size and image quality, and several images were used per datapoint. The standard deviation (STD) of each calculated value expresses the measurement error rooted in the analysis of the STM images.

Results and Discussion

Figure 2 shows the molecule arrangement for a single layer of coronene on HOPG, and the corresponding FFT (Fast Fourier Transform) pattern, which reflects the hexagonal symmetry. The images in Figure 2 were recorded with different V_b probing the empty states of molecules and substrate. The image taken $V_b = 1.2$ V is dominated by the molecule signal. Figure 2b, on the other hand, displays a fine structure, which is likely dominated by contributions from the HOPG substrate since at $V_b = 0.1$ V only states within the band gap of coronene ($E_g = 2.4$ eV) can be probed. At the same time the relatively high feedback current of 1 nA used in these measurements positions the tip close to the surface thus increasing the contribution from HOPG to the tunneling current. In the FFT pattern the signature of the hexagonal lattice from the molecule overlayer, and the FFT signature of the intra-molecular structure, which is positioned at larger inverse distance values in the FFT, are rotated by about $\sim 12°$ with respect to each other. This is in agreement with the previously reported $\sqrt{21} \times \sqrt{21}R \pm 10.9°$ superstructure of coronene on HOPG(0001).[17,39] and confirms that the image recorded at $V_b = 0.1$ V shows the underlying graphite surface, superposed on the coronene surface layer structure.

The coronene layer on Au(111) (Cor/Au(111)), is shown in Figure 3 prior to annealing: the molecules do not preferentially adsorb at specific bonding sites defined by the Au(111) herringbone reconstruction, which was confirmed prior to deposition, due to the relatively weak molecule-substrate interaction.[40,41] The unit cell is marked in Figure 3b. The lattice constant of 1.15 nm confirms the 4×4 commensurate layer structure where the molecules lie flat on the surface.[26] Deposition of the molecules at RT was followed by annealing to a maximum of 116°C and a representative selection of images is assembled in Figure 4. Some images show sections with artifacts from streaks such as in the bottom section of Figure 4a, and 4b, which are not unusual in molecule imaging, and these regions are excluded from the statistical analysis. 4c is measured after annealing to 116°C. This temperature is below the multilayer desorption temperature, and avoids any decomposition of the molecule.[19] The

initial coverage is chosen to achieve a complete 1st layer with very sparse 2nd layer islands.

Imaging the same sample with $V_b = 1.2$ V and a smaller tunneling current of 0.05 nA on rare occasion delivered an image such as the one shown in Figure 4d. Figure 4d is near identical to the STM images of coronene molecules on Ag(111) presented in[22] which were interpreted as tilted molecules in agreement with tilt of about 16° given by Yannoulis et al.[23] The linescan on the right hand side of the image seems to support this interpretation where the smaller protrusion on the left hand side of individual molecule images might correspond to one benzene ring where the π bonded system interacts most strongly with the substrate. However, the unusual image contrast can equally well be explained by the modification of the tip by termination with a coronene molecule introducing an asymmetric appearance in the images. This image was not included in the statistical image analysis discussed in the next paragraph.

Figure 5 summarizes the results of the statistical analysis as a function of annealing temperatures for Cor/Au(111) and includes the distributions of molecule radii (distance from the molecule center to boundary), and intermolecular distance measured from maximum-to-maximum. All data included in this analysis were measured with identical $V_b = 1.2$ V. The position of maxima and minima are determined using the method described in the Data Analysis section. The molecule radii histograms reflect the hexagonal shape of the molecule envelope and the smallest radii of about 0.55 nm correspond to the apothem r (incircle radius) of the molecule envelope, while the longest distances of about 0.75 nm corresponds to the circumcirle radius R and agrees with the geometric relation defined by the hexagon shape. The radii as a function of temperature shown on the right hand side of the figure use the maxa of the radius histograms. The distribution of radii as well as the distribution of intermolecular distances are not modified by annealing, and Cor/Au(111) and Cor(HOPG) layers are identical within the measurement error. This is summarized in Figure 5c - d.

The next analysis step, the assessment of molecule height, is illustrated in Figure 6. The height of a coronene molecule in a monolayer measured with STM was previously reported

as ∼0.05 to 0.1 nm[2,27 30] and our apparent heights are within this range with 0.09 nm±0.012 nm. All images used in this analysis were measured with the same bias voltage, and a small tunneling current 0.12 ± 0.08 nA. Details of the apparent height measurement for Cor/Au(111) as a function of bias voltage will be addressed in the next section. The apparent molecule height is, for a closed layer, the height differential between the aromatic rings defined by the π-orbitals extending above the plane of the molecules, and the σ-bonded hydrogen terminated perimeter. The total height of a coronene molecule is ∼0.3 nm,[28] albeit in the images of a closed layer we only measure the apparent height differential between molecule center and top of the hydrogen terminated rim. The apparent height measured with STM within the layer is nearly constant at lower temperatures, but increases three fold in the final anneal step at 116°C. The representative linescans in Figure 6b - c underscore this result: they were measured along three different directions in the as-deposited sample and after the final anneal. Before annealing the apparent height in all directions is identical within the precision of the measurement, while this is not the case for linescans recorded after the anneal. The statistical analysis of the images, which followed the method illustrated in Figure 1, delivers a reliable average value for the modulation of apparent height.

Height measurements in STM always present a convolution of LDOS (local density of states) and topography information, and the variation of the apparent height in Cor/Au(111) images was therefore assessed independently. Figure 7 summarizes the spectroscopy data, images, and apparent height measurements as a function of V_b after the 116°C anneal. Image quality was generally poor for $V_b < 0.6$ V. The normalized differential conductance, which is proportional to the LDOS, is displayed for single and multilayer islands in Figure 7a, and indicates a p-type doping in the monolayer, and neutral position of the Fermi energy for multilayers. The multilayer coronene island has the full band gap of 2.4 eV, while the monolayer has a reduced band gap of about 1.5 eV due to the interaction of the molecule frontier orbitals with the d-electron system of the metal.[42–44] The apparent height is constant for $V_b < 2.0$ V, which confirms that a suitable bias voltage was selected for the statistical

analysis. The unreliable imaging for lower bias voltage is due to tunneling into the bandgap of the coronene layer. The reduced apparent height difference observed at higher bias voltage exceeding 2.0 V reflects the variation in the local density of states between the rim and the aromatic molecule center, which could not be resolved individually. Going back to Cor/HOPG the importance of checking for the apparent height is evident - in Figure 2 the molecules are depressions for $V_b = 1.2$ V but protrusions for $V_b = 0.1$ V due to the contributions from the LDOS of molecules or the substrate.[17,39] It remains an open question why such a contrast inversion is not seen in the Cor/Au(111) system but might be attributed to a weak hybridization between the coronene frontier orbital and the d-band of the Au-substrate although the desorption energies for both systems from the monolayer are similar.[45]

The image analysis, and specifically the height analysis, support a tilting of the molecules at the highest annealing temperature. Warping or other complex deformation scenarios are not accessible within our experimental resolution. A moderate buckling with a 10° angle at the attachment point at the molecule perimeter with respect to the detached center yields only a small decrease in molecule radius by 4%, and a height increase at the center by 0.1 nm or at most 17% of the molecule radius. These values are smaller than the measured height variation, although it could be argued that the apparent height might be modified by lifting the molecule center off the Au-substrate due to a local change in LDOS. Molecular buckling has only been observed in coronene systems with strong molecule-substrate interaction such as Cor/Si[13] and Cor/Rh[2] since the molecule substrate interaction has to balance the loss in aromaticity due to buckling. However, buckling should not be discarded as a possible explanation for the relatively subtle variations in molecule arrangement.

A simple geometric argument can be made to obtain an estimate of the tilt angle θ for the molecules with respect to the Au(111) surface plane. Figure 8 shows the calculated effective molecule diameter d_{eff} - corresponding to the molecule dimension as measured with STM as a function of tilt - and the molecule height h_{eff} and assumes that the molecules tilt but

do not significantly overlap as shown in the sketch included in the Figure:

$$d_{eff} = d_{cor} cos(\theta) \tag{1}$$

$$h_{eff} = d_{cor} sin(\theta) + h_{cor} \tag{2}$$

for the case of non-overlapping molecules. h_{cor} is set at 0.1 nm, and d_{cor} at 1.15 nm. The effective molecule diameter changes indeed very little at low tilt angles and this minute variation is difficult to detect experimentally. In contrast, the molecule height increases significantly even at low tilt angles. Any tilt angle of less than 20° will only be recognized by a variation in molecule height, but not in a change in effective molecule diameter. The molecule height observed in the as-deposited layers, and the last annealing step are marked as gray bars whose width corresponds to the experimental error. This estimate yields a tilt angle of 11±4°/ Small tilt angles are therefore accessible with good precision if a large number of molecules is included in the analysis. The line scans agree with this tilt angle albeit have a much larger margin of error due to the smaller number of datapoints. In conclusion, monolayer coronene on Au(111) is flat after deposition, and adopts a small molecule tilt without or only very small overlap between the molecules after annealing to 116°C.

Coronene molecules arriving on the Au surface will preferentially adsorb with their π bonded system flat on the surface, which is the most common adsorption geometry for simple aromatic molecules such as benzene, and polycyclic aromatic hydrocarbons.[46,47] The weak interaction between Au and coronene still allows for diffusion and formation of a densely packed molecular layer with hexagonal symmetry as seen here. Structural variations in molecular layers are frequent and subject to often small variations in interaction potentials such as Cor/Ag(110).[25] The slightly tilted arrangement is therefore tentatively interpreted as metastable configuration in analogy to the recently reported assessment of Cor/Cu(111). The molecules are still tethered to the Au(111) surface through the interaction between the molecule π electron system and the Au d-band/electronic surface states. The tilt for

Cor/Au(111) is smaller then for either Cor/Ag(111) or Cor/Cu(111) and a theoretical assessment of interaction potentials might in the future shed light on the differences.

Tilt is generally related to the density of the molecule layer, and a higher density such as it is achieved in a full monolayer, promotes the onset of molecule tilting as an intermediate to the bulk-type stacking with optimized van der Waals interactions between the molecules in the bulk material. We propose that for the Cor/Au(111) system the differences thermal expansion coefficient between bulk coronene, which exceed the value for Au by more than an order of magnitude, is sufficient to trigger the onset of tilting through densification of the molecule layer.[48] Thermal expansion coefficients[48] have their origin in the anharmonicity of the molecule-molecule interaction potential, and hence the difference in thermal expansion between Au and coronene is expected to hold even if the exact values might differ in thin molecular layers compared to measured bulk values. Annealing introduces strain in the coronene layer, which is accommodated by tilting of the molecules.

The measured tilt angle of about 11° yields a distance between Au surface and the elevated side of the molecule of about 0.17 nm, which is not enough space to allow for a coronene molecule to slip beneath the adjacent molecule. It is possible that the stacking is more extreme with a larger tilt angle during heating and the molecule structure partially relaxes after cooling to room temperature. However, energy barriers due to steric constraints are likely to be small considering the geometry of the coronene molecule, and we therefore propose an alternative interpretation for the retention of tilt based on the work by Medeiros et al.[47] The tilt once initiated is stabilized by the bonding between the hydrogen-terminated molecule perimeter and the Au substrate. Medeiros et al. illustrated in their comparison of bonding for different aromatic molecules from benzene to coronene and graphene, that C-H groups bind more strongly to the Au(111) surface than the internal C-C bonds. A slight tilt is consequently supported, and sustained, through the favorable C-H/Au(111) bonding configuration.

Conclusion

Coronene on Au(111) surfaces adsorbs in a flat orientation at room temperature, and the molecules tilt after annealing to 116°C. STM/STS measurements of Cor/Au(111) in combination with the use of automated image analysis provide the basis for this observation. The combination of experiment with image analysis software is a powerful tool in the study of small modulations of molecule layer structure, which are very hard to detect based solely on individual linescans. Image analysis software allows us to make full use of all parts of an image and provides a statistically relevant database for interpretation of physical phenomena. A successful implementation of the analysis routines requires high quality images, and assessment of apparent height as a function of bias voltage to avoid introduction of artifacts in the height analysis. Ideally all images will be recorded with identical (or near identical) imaging parameters. For future work in the study of small modulations of images it might be useful to quantify instrument specific image distortions in a separate measurement.In conclusion, we have demonstrated that even small variations in molecule structure can be assessed in a quantitative manner by combining STM/STS experiments with automated image analysis.

Acknowledgement

We acknowledge the support from the National Science Foundation award CHE-1507986 by the Division of Chemistry (Macromolecular, Supramolecular and Nanochemistry). Statement of Work: N.K. and P.R conceived the experiment, N.K performed the experiments with assistance from E.M. N.K and P.R did the data analysis and wrote the manuscript. Data from this work is stored on Libra, the University of Virginia's institutional repository. Please contact Professor Petra Reinke about gaining access to additional information and the data presented in this manuscript.

References

(1) Coraux, J.; N'Diaye, A. T.; Engler, M.; Busse, C.; Wall, D.; Buckanie, N.; Heringdorf, F.-J. M. z.; van Gastel, R.; Poelsema, B.; Michely, T. Growth of graphene on Ir(111). *New Journal of Physics* **2009**, *11*, 035024–23.

(2) Wang, B.; Ma, X.; Caffio, M.; Schaub, R.; Li, W.-X. Size-Selective Carbon Nanoclusters as Precursors to the Growth of Epitaxial Graphene. *Nano Letters* **2011**, *11*, 424–430.

(3) Wu, T.; Ding, G.; Shen, H.; Wang, H.; Sun, L.; Zhu, Y.; Jiang, D.; Xie, X. Continuous graphene films synthesized at low temperatures by introducing coronene as nucleation seeds. *Nanoscale* **2013**, *5*, 5456–6.

(4) Cui, Y.; Fu, Q.; Zhang, H.; Bao, X. Formation of identical-size graphene nanoclusters on Ru(0001). *Chemical Communications* **2011**, *47*, 1470–1472.

(5) Chang, S.; Liu, R.; Wang, L.; Li, M.; Deng, K.; Zheng, Q.; Zeng, Q. Formation of Ordered Coronene Clusters in Template Utilizing the Structural Transformation of Hexaphenylbenzene Derivative Networks on Graphite Surface. *ACS Nano* **2016**, *10*, 342–348.

(6) Dai, H.; Yi, W.; Deng, K.; Wang, H.; Zeng, Q. Formation of Coronene Clusters in Concentration and Temperature Controlled Two-Dimensional Porous Network. *ACS Applied Materials & Interfaces* **2016**, *8*, 21095–21100.

(7) Wu, X.; Xu, C.; Wang, K.; Xiao, X. Charge Transfer, Phase Separation, and Mott–Hubbard Transition in Potassium-Doped Coronene Films. *The Journal of Physical Chemistry C* **2016**, *120*, 15446–15452.

(8) Yano, M.; Endo, M.; Hasegawa, Y.; Okada, R.; Yamada, Y.; Sasaki, M. Well-ordered monolayers of alkali-doped coronene and picene: Molecular arrangements and electronic structures. *The Journal of Chemical Physics* **2014**, *141*, 034708–8.

(9) Wiebner, M.; Lastra, N. S. R.; Ziroff, J.; Forster, F.; Puschnig, P.; Dossel, L.; Mullen, K.; Scholl, A.; Reinert, F. Different views on the electronic structure of nanoscale graphene: aromatic molecule versus quantum dot. *New Journal of Physics* **2012**, *14*, 262001–13.

(10) Wang, C.; Thuermer, K.; Skeen, S.; Bartelt, N. C. When do hydrocarbons dewet metal surfaces? The case of coronene on Cu(111). *Surface Science* **2020**, 121603.

(11) Robertson, J. M.; White, J. G. The crystal structure of coronene: a quantitative X-ray investigation. *Journal of the Chemical Society (Resumed)* **1945**, 607–11.

(12) Igor, F.; Yurii, Z.; Victor, B. Properties of crystalline coronene: Dispersion forces leading to a larger van der Waals radius for carbon. *physica status solidi (b) 249*, 1438–1444.

(13) Suzuki, T.; Sorescu, D. C.; Jordan, K. D.; Levy, J.; Yates Jr., J. T. The chemisorption of coronene on Si(001)-2x1. *The Journal of Chemical Physics* **2006**, *124*, 054701–7.

(14) Martínez-Blanco, J.; Klingsporn, M.; Horn, K. Selective adsorption of coronene on Si(111)-(7x7). *Surface Science* **2010**, *604*, 523–528.

(15) Martínez-Blanco, J.; Mascaraque, A.; Dedkov, Y. S.; Horn, K. Ge(001) As a Template for Long-Range Assembly of π-Stacked Coronene Rows. *Langmuir* **2012**, *28*, 3840–3844.

(16) Martínez-Blanco, J.; Walter, B.; Mascaraque, A.; Horn, K. Long-Range Order in an Organic Overlayer Induced by Surface Reconstruction: Coronene on Ge(111). *The Journal of Physical Chemistry C* **2014**, *118*, 11699–11703.

(17) Walzer, K.; Sternberg, M.; Hietschold, M. Formation and characterization of coronene monolayers on HOPG(0001) and MoS2(0001): a combined STM/STS and tight-binding study. *Surface Science* **1998**, *415*, 1–9.

(18) Dappe, Y. J.; Andersen, M.; Balog, R.; Hornekær, L.; Bouju, X. Adsorption and STM imaging of polycyclic aromatic hydrocarbons on graphene. *Physical Review B* **2015**, *91*, 045427–8.

(19) Thrower, J. D.; Friis, E. E.; Skov, A. L.; Nilsson, L.; Andersen, M.; Ferrighi, L.; Jørgensen, B.; Baouche, S.; Balog, R.; Hammer, B.; Hornekær, L. Interaction between Coronene and Graphite from Temperature-Programmed Desorption and DFT-vdW Calculations: Importance of Entropic Effects and Insights into Graphite Interlayer Binding. *The Journal of Physical Chemistry C* **2013**, *117*, 13520–13529.

(20) England, C. D.; Collins, G. E.; Schuerlein, T. J.; Armstrong, N. R. Epitaxial Thin Films of Large Organic Molecules: Characterization of Phthalocyanine and Coronene Overlayers on the Layered Semiconductors MoS2 and SnS2. *Langmuir* **2001**, *10*, 1–9.

(21) Huempfner, T.; Sojka, F.; Forker, R.; Fritz, T. Growth of coronene on (100)- and (111)-surfaces of fcc-crystals. *Surface Science* **2015**, *639*, 80–88.

(22) Lackinger, M.; Griessl, S.; Heckl, W. M.; Hietschold, M. Coronene on Ag(111) Investigated by LEED and STM in UHV. *The Journal of Physical Chemistry B* **2002**, *106*, 4482–4485.

(23) Yannoulis, P.; Dudde, R.; Frank, K. H.; Koch, E. E. Orientation of aromatic hydrocarbons on metal surfaces as determined by NEXAFS. *Surface Science* **1987**, *87*.

(24) Udhardt, C.; Otto, F.; Kern, C.; Lüftner, D.; Huempfner, T.; Kirchhuebel, T.; Sojka, F.; Meissner, M.; Schröter, B.; Forker, R.; Puschnig, P.; Fritz, T. Influence of Film and Substrate Structure on Photoelectron Momentum Maps of Coronene Thin Films on Ag(111). *The Journal of Physical Chemistry C* **2017**, *121*, 12285–12293.

(25) Shi, D.; Ji, W.; Yang, B.; Cun, H.; Du, S.; Chi, L.; Fuchs, H.; Hofer, W. A.; Gao, H.-J. Alternating the Crystalline Structural Transition of Coronene Molecular Overlayers on

Ag(110) through Temperature Increase. *The Journal of Physical Chemistry C* **2009**, *113*, 17643–17647.

(26) Seidel, C.; Ellerbrake, R.; Gross, L.; Fuchs, H. Structural transitions of perylene and coronene on silver and gold surfaces: A molecular-beam epitaxy LEED study. *Physical Review B* **2001**, *64*, 195418–10.

(27) Yoshimoto, S.; Narita, R.; Wakisaka, M.; Itaya, K. The structure of a coronene adlayer formed in a benzene solution: studies by in situ STM and ex situ LEED. *Journal of Electroanalytical Chemistry* **2002**, 1–5.

(28) English, W. A.; Hipps, K. W. Stability of a Surface Adlayer at Elevated Temperature: Coronene and Heptanoic Acid on Au(111). *The Journal of Physical Chemistry C* **2008**, *112*, 2026–2031.

(29) Jahanbekam, A.; Vorpahl, S.; Mazur, U.; Hipps, K. W. Temperature Stability of Three Commensurate Surface Structures of Coronene Adsorbed on Au(111) from Heptanoic Acid in the 0 to 60°C Range. *The Journal of Physical Chemistry C* **2013**, *117*, 2914–2919.

(30) Gyarfas, B. J.; Wiggins, B.; Zosel, M.; Hipps, K. W. Supramolecular Structures of Coronene and Alkane Acids at the Au(111)-Solution Interface: A Scanning Tunneling Microscopy Study. *Langmuir* **2005**, *21*, 919–923.

(31) Yoshimoto, S.; Tsutsumi, E.; Fujii, O.; Narita, R.; Itaya, K. Effect of underlying coronene and perylene adlayers for [60]fullerene molecular assembly. *Chemical Communications* **2005**, 1188–3.

(32) Yoshimoto, S.; Tsutsumi, E.; Narita, R.; Murata, Y.; Murata, M.; Fujiwara, K.; Komatsu, K.; Ito, O.; Itaya, K. Epitaxial Supramolecular Assembly of Fullerenes Formed by Using a Coronene Template on a Au(111) Surface in Solution. *Journal of the American Chemical Society* **2007**, *129*, 4366–4376.

(33) Udhardt, C.; Otto, F.; Kern, C.; Lüftner, D.; Huempfner, T.; Kirchhuebel, T.; Sojka, F.; Meissner, M.; Schröter, B.; Forker, R.; Puschnig, P.; Fritz, T. Influence of Film and Substrate Structure on Photoelectron Momentum Maps of Coronene Thin Films on Ag(111) . *The Journal of Physical Chemistry C* **2017**, *121*, 12285–12293.

(34) Horcas, I.; Fernández, R.; Gómez-Rodríguez, J. M.; Colchero, J.; Gómez-Herrero, J.; Baro, A. M. WSXM: A software for scanning probe microscopy and a tool for nanotechnology. *Review of Scientific Instruments* **2007**, *78*, 013705–9.

(35) Nečas, D.; Klapetek, P. Gwyddion: an open-source software for SPM data analysis. *Open Physics* **2011**, *10*, 99–8.

(36) Stirling, J.; Woolley, R. A. J.; Moriarty, P. Scanning probe image wizard: A toolbox for automated scanning probe microscopy data analysis. *Review of Scientific Instruments* **2013**, *84*, 113701–7.

(37) Zevenhuizen, S. J. M. SPIEPy: Scanning Probe Image Enchanter using Python. **2014**,

(38) Pedregosa, F.; Varoquaux, G.; Gramfort, A.; Michel, V.; Thirion, B.; Grisel, O.; Blondel, M.; Prettenhofer, P.; Weiss, R.; Dubourg, V.; Vanderplas, J.; Acuna, M. H.; Passos, A.; Cournapeau, D. Scikit-learn: Machine Learning in Python. *Journal of Machine Learning Research* **2011**, 1–6.

(39) Zimmermann, U.; Karl, N. Epitaxial growth of coronene and hexa-peri-benzocoronene on MoS2(0001) and graphite (0001): a LEED study of molecular size effects. *Surface Science* **1992**, *268*, 296–306.

(40) Yokoyama, T.; Yokoyama, S.; Kamikado, T.; Okuno, Y.; Mashiko, S. Selective assembly on a surface of supramolecular aggregates with controlled size and shape. *Nature* **2001**, *413*, 619–621.

(41) Maksymovych, P.; Sorescu, D. C.; Dougherty, D.; Yates, J. T. Surface Bonding and Dynamical Behavior of the CH 3SH Molecule on Au(111). *The Journal of Physical Chemistry B* **2005**, *109*, 22463–22468.

(42) Neaton, J. B.; Hybertsen, M. S.; Louie, S. G. Renormalization of Molecular Electronic Levels at Metal-Molecule Interfaces. *Physical Review Letters* **2006**, *97*, 98–4.

(43) Monazami, E.; McClimon, J. B.; Rondinelli, J.; Reinke, P. Electronic Structure and Band Gap of Fullerenes on Tungsten Surfaces: Transition from a Semiconductor to a Metal Triggered by Annealing. *ACS Applied Materials & Interfaces* **2016**, *8*, 34854–34862.

(44) McClimon, J. B.; Monazami, E.; Reinke, P. Interaction of C 60with Tungsten: Modulation of Morphology and Electronic Structure on the Molecular Length Scale. *The Journal of Physical Chemistry C* **2014**, *118*, 24479–24489.

(45) Chilukuri, B.; Mazur, U.; Hipps, K. Cooperativity and coverage dependent molecular desorption in self-assembled monolayers: computational case study with coronene on Au (111) and HOPG. *Physical Chemistry Chemical Physics* **2019**, *21*, 10505–10513.

(46) Nishiyama, K.; Harada, H.; Yoshimoto, S.; Taniguchi, I.; Yamada, T. HREELS Evaluation of Coronene Monolayer Adsorption on Au (111) as the First Base Layer to Achieve Coordination Programming. *Chemistry Letters* **2014**, *43*, 1340–1342.

(47) Medeiros, P. V.; Gueorguiev, G. K.; Stafström, S. Benzene, coronene, and circumcoronene adsorbed on gold, and a gold cluster adsorbed on graphene: Structural and electronic properties. *Physical Review B* **2012**, *85*, 205423.

(48) Litasov, K. D.; Gavryushkin, P. N.; Yunoshev, A. S.; Rashchenko, S. V.; Inerbaev, T. M.; Akilbekov, A. T. Thermal expansion of coronene C24H12 at 185–416 K. *Journal of Thermal Analysis and Calorimetry* **2014**, *119*, 1183–1189.

Figures

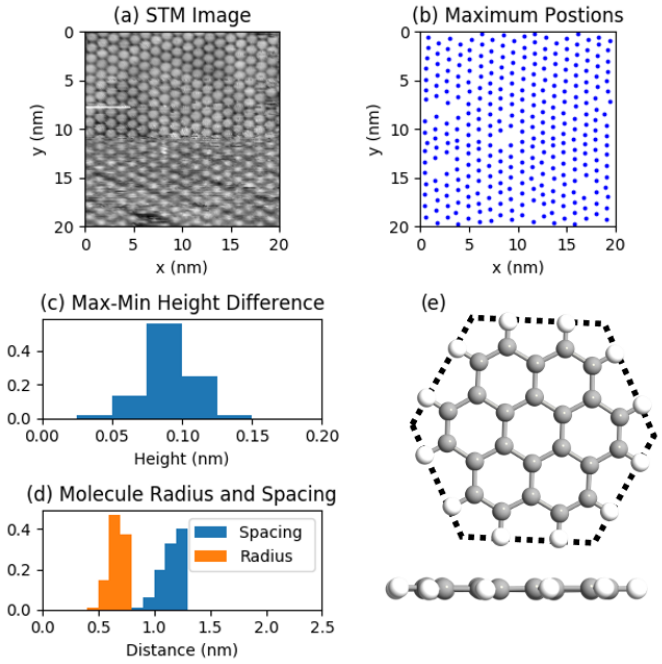

Figure 1: Example of Cor/Au(111) and the maximum and minimum positions are located by the SPIEPy algorithms. Maxima and minima correspond to high and low tunneling currents, respectively. (A) STM image for Cor/Au(111) as deposited, (b) position of maxima located by SPIEPy in the STM image, (c) histogram of height values as the difference between maxima and minima in apparent height, (d) histogram of intermolecular spacing (max-max distance), and molecule radius (max-min distance), and (e) Ball and stick model of the coronene molecule. Histograms are normalized to unit height.

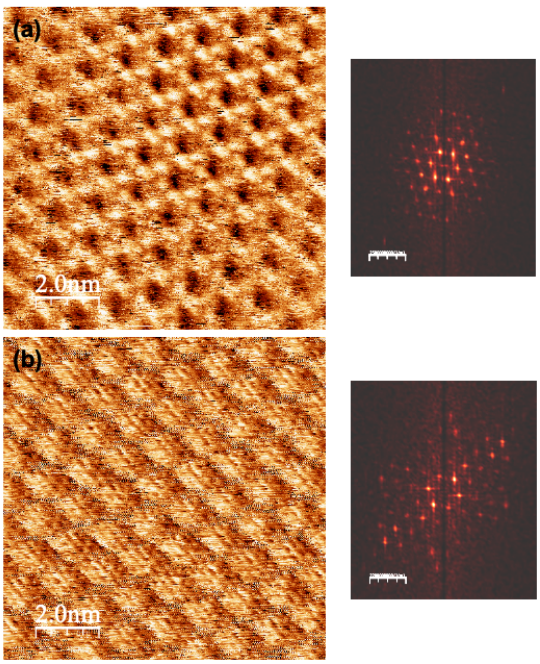

Figure 2: STM images of coronene on HOPG (10×10 nm) and the corresponding FFT patterns. Imaging conditions for (a) are V_b=1.2 V, I_t = 0.18 nA, scale bar FFT 2.5 1/nm, and for (b) V_b=0.1, I_t= 1 nA, scale bar FFT 2.2 1/nm.

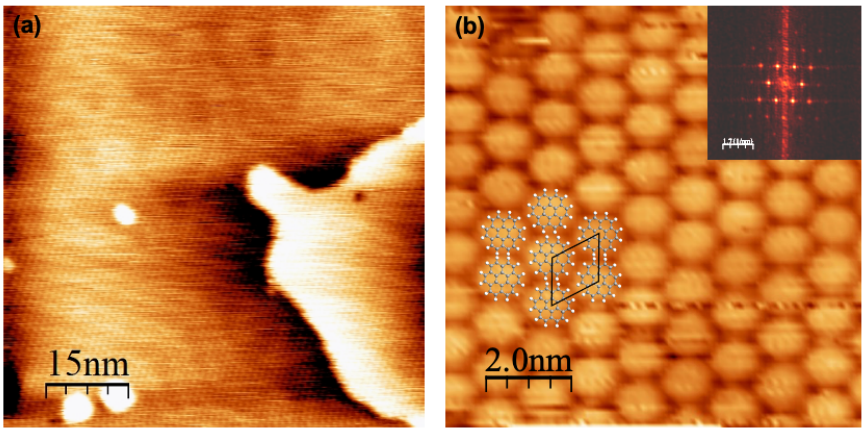

Figure 3: (a) STM image (V_b = 1.2 V, I_t = 0.18 nA) of coronene molecules adsorbed on the Au(111) surface. The herringbone reconstruction of the Au-substrate is visible through the molecule adlayer. (B) Higher resolution STM image (V_b=1.2 V, I_t=0.1 nA) of coronene molecules on the Au(111) surface. The molecule structure is superimposed on the image, and the inset shows the corresponding FFT pattern (scale bar 1.7 1/nm). Both images were taken before annealing.

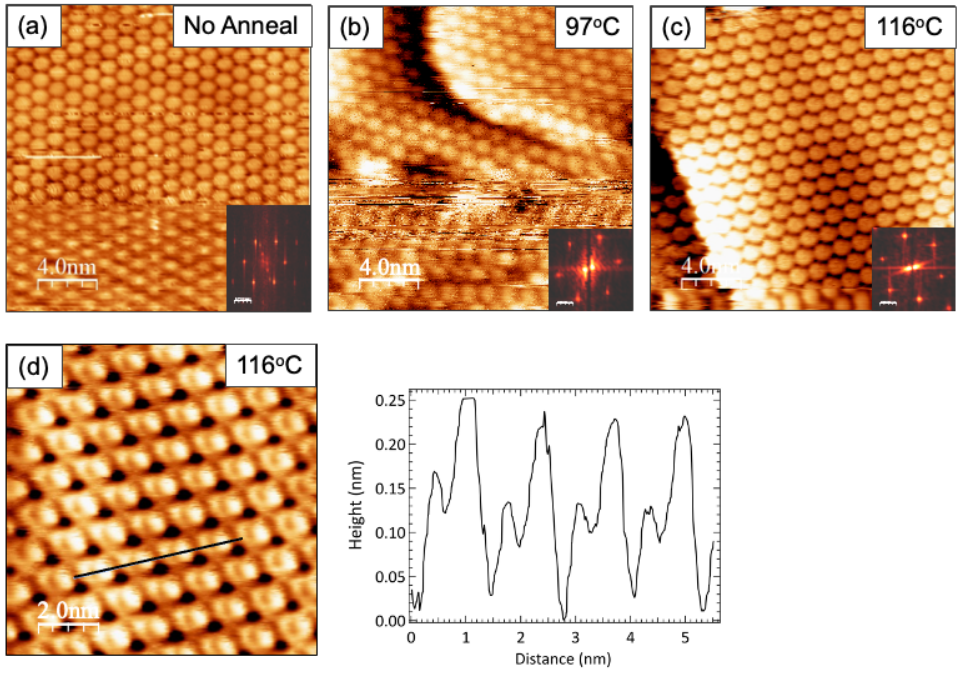

Figure 4: STM images after annealing steps (a) as deposited, (b) 97°C anneal, and (c) 116°C anneal. These images are 20×20 nm, and $V_b = 1.2$ V, $I_t = 0.1$ nA. (d) after 116°C anneal measured with $V_b = 1.2$ V, $I_t = 0.05$ nA; image size 10×10 nm

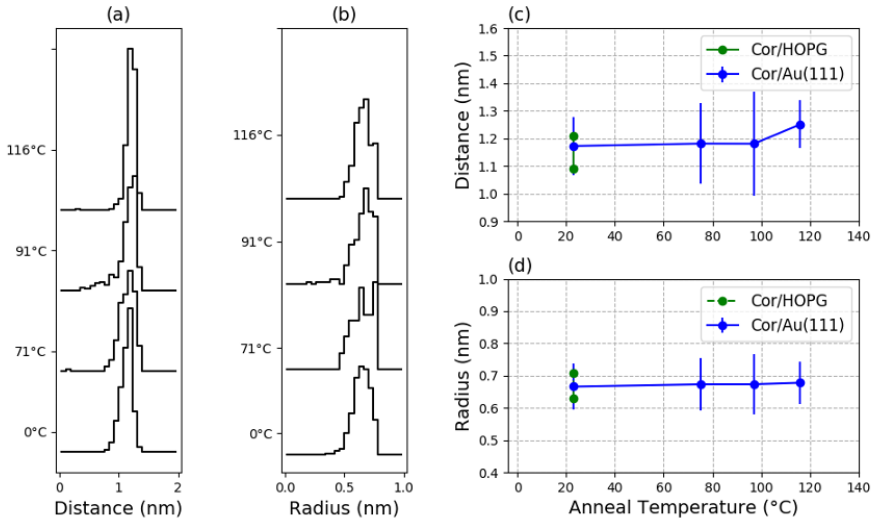

Figure 5: Summary of molecule spacing and radius variations as a function of anneal temperature. (a) Histograms of intermolecule distance), (b) histograms of molecule radii, (c) average values for molecule distance versus anneal temperature, (d) average values of molecule radii versus anneal temperature. Data for Cor/Au(111) and Cor/HOPG are included. Histograms are normalized to unit height.

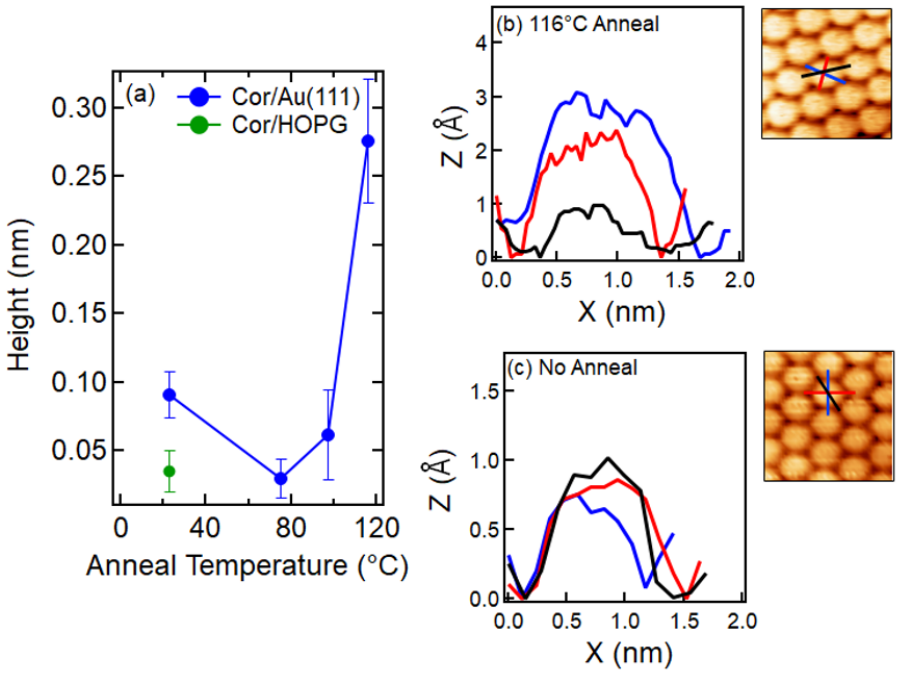

Figure 6: (a) Summary of molecule height variations with anneal temperature for Cor/Au(111), and room temperature data for Cor/HOPG, (b) typical linescans across molecule after 116°C anneal for Cor/Au(111), and (c) typical linescans across a molecule before anneal on Cor/Au(111).

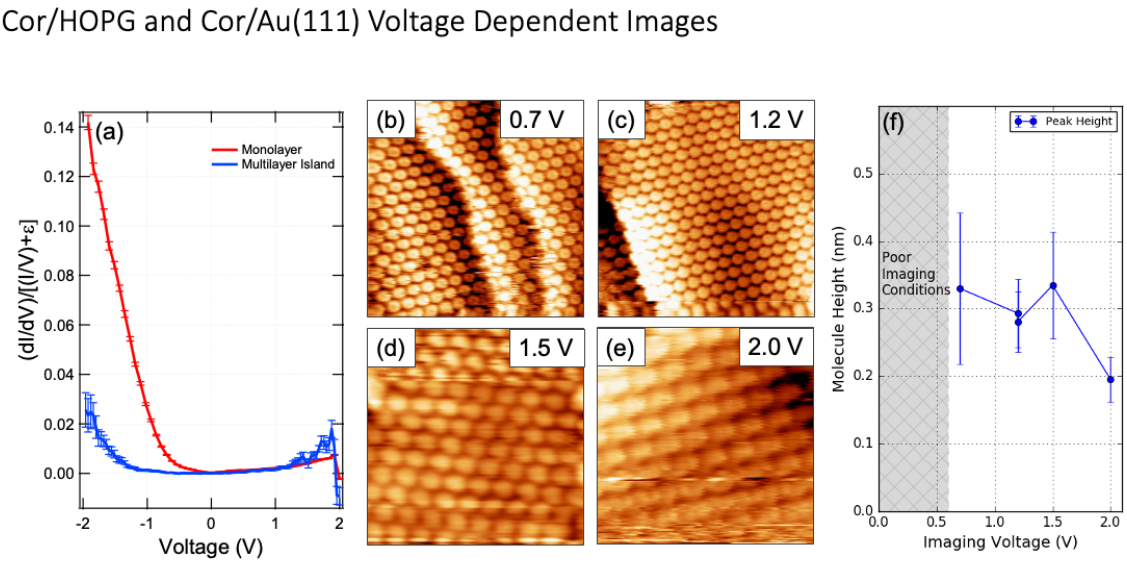

Figure 7: (a) Normalized ST spectra (dI/dV)[(I/V)] from a coronene monolayer after anneal 116°C, and a small patch of multilayer coronene island on Au(111).
Voltage dependent STM images of Cor/Au(111) after the anneal to 116°C: (b) 20×20 nm at V_b=0.7 V, (c) 20×20 nm at V_b=1.2 V, (d) 15×15 nm at V_b=1.5V, and (e) 10×10 nm at V_b=2 V. (f) summarizes the apparent molecule height difference between molecule center and hydrogen terminated rim in between molecules as a function of bias voltage. Any imaging below ∼0.6 V resulted in poor image quality.

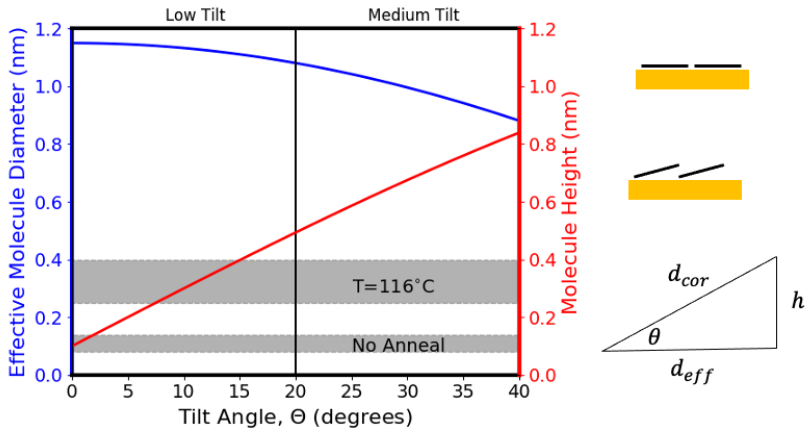

Figure 8: Summary of the geometric tilting model for Cor/Au(111) comparing the variation in effective molecule diameter and molecule height with molecule tilt angle measured with respect to the Au(111) surface plane. Gray bars represent corresponding molecule height measured from STM images for (a) no anneal and (b) 116°C anneal and the width of the bar corresponds to the measurement error.